The flux densities of some radio sources at 400 Mc/s

Seeger, C.L.; Westerhout, G.; Hulst, H.C. van de

BULLETIN OF THE ASTRONOMICAL INSTITUTES OF THE NETHERLANDS

1956 NOVEMBER 26 VOLUME XIII NUMBER 472

COMMUNICATIONS FROM THE NETHERLANDS FOUNDATION FOR RADIO ASTRONOMY AND THE OBSERVATORY AT LEIDEN

THE FLUX DENSITIES OF SOME RADIO SOURCES AT 400 Mc/s

BY CH. L. SEEGER, G. WESTERHOUT AND H. C. VAN DE HULST

Observations of some discrete radio sources and the surrounding regions were made with a 25-metre telescope at 400 M c/s. The beam width was about 2°.
Regional isophote maps of four regions including several of the major discrete sources are given (Figures 1-4). Flux densities of these and other sources are given in Table 5. They have been corrected for receiver alinearity, extinction and finite size. The ratios of the flux densities of the four strongest sources have been determined with an accuracy of a few per cent by a method of rapid intercomparison. The absolute values are based on a tentative measurement of the Cas source described in a separate paper. Rough estimates of the brightness temperature of the galactic background in various directions are given in Table 6. Scintillation was observed when the sources were at low altitude. It was stronger and faster on one night of enhanced geomagnetic activity. An *appendix* summarizing the terms and formulae used in the reduction may be of general use for the reduction of observations taken with narrow-beam antennas.

1. *Equipment and programme*

A 400 Mc/s receiver and circular wave-guide feed were temporarily installed in the 25-metre paraboloid at Dwingeloo at the occasion of the occultations of the Crab nebula [1]) by the moon on Nov. 3 and 30, 1955. The equipment was tested during several days before each date by observations on strong point sources and on some interesting regions of the sky. The results of these side programmes are reported in this paper.

At the second date construction work had advanced far enough to allow setting in both co-ordinates. Temporary scales of altitude and azimuth were calibrated within 0°.1 on strong point sources. At the first date the telescope had a fixed elevation of 2°; observations up to 7° elevation were possible by lowering the mast supporting the feed. All co-ordinate conversions were made by desk computation, as the pilot was not yet in operation.

In reducing the records we employed provisional units corresponding to 1 unit on the 100 mV scale (of detector output) at the receiver sensitivity of Nov. 30. One unit is equivalent to 1°.26 net antenna temperature (p. 90). The noise on the records was such that an accuracy of about 4 units could be obtained in a single setting on a source during 2 minutes. This is one per cent of Cyg A and less than one per cent of Cas A. Slow variations affecting the final accuracy are due to a variety of causes, among which are the changing wind conditions affecting the temperature of the r.f. amplifier and first mixer that were housed in a wooden box on the platform behind the vertex of the paraboloid.

The North pole was used as a reference point to determine receiver drifts. Typical drift values were 3 or 5 units in ten minutes; the estimated uncertainty of the interpolated North pole values is 2 units.

2. *Corrections and conversion factors*

The reduction involves a number of corrections that may be briefly described here.

Alinearity. The detector law was determined several times in the course of these measurements. This was done by replacing the antenna by a dummy load and inserting attenuations, by steps of 1 db, in the i.f. amplifier. Let $W = W_1 + P$ be the input power of the detector in arbitrary units and let $E = E_1 + r$ be

[1]) Ch. L. SEEGER, *B.A.N.*, to be published.

CONTENTS

the output voltage of the detector in the units used above, and counted from the usual zero at $W = 0$. Further, let W_1 and E_1 be the values that hold when the antenna is pointing to the North pole, so that r is the reading above the North pole level. The detector law may be represented by $W \sim E^\alpha$ in the measuring range (2 db in W). If the units of P are chosen to have $P = r$ for small increments, we have $P = p.r$ for arbitrary increments, where the factor p is given by

$$p = \frac{(1+u)^\alpha - 1}{\alpha u} =$$
$$= 1 + \tfrac{1}{2}(\alpha - 1)u + \tfrac{1}{6}(\alpha - 1)(\alpha - 2)u^2 + \ldots,$$

where $u = r/E_1$.
The present data are $\alpha = 1.33$, $E_1 = 1650$ units. The average reading on Cas A was 512 units, giving $p = 1.048$. The alinearity correction is smaller for the weaker sources.

Extinction. As suitable measurements for determining the extinction coefficient were not made during these tests, a theoretical value was employed in the reduction, VAN VLECK[1]) gives

$$\gamma = \frac{C\nu^2\,\Delta\nu}{\nu^2 + \Delta\nu^2}\ \text{db/km}$$

for nonresonant absorption by O_2 molecules, which he shows to be the only effect at these wavelengths. Here ν = wave number in cm^{-1}, $\Delta\nu$ = line-broadening coefficient in cm^{-1}. The numerical estimates for air at atmospheric pressure and $T = 293°$ are $C = 0.34$, $\Delta\nu = 0.02$, which give $\gamma = 0.0021$ db/km at 400 Mc. This result happens to be fairly insensitive to variations in the assumed $\Delta\nu$. It may be estimated that the entire atmosphere corresponds to about 10 km of the atmospheric air of VAN VLECK's examples. The extinction value of 0.02 db at the zenith was, therefore, used in the reductions. It corresponds to $\varepsilon = 0.0046 \operatorname{cosec} h$ (A 21)[2]).

The extinction observed at 21 cm, which is 0.042 ± .003 db at the zenith[3]), is not far below the value computed from VAN VLECK's formula.

Conversion factors. The extraterrestrial flux density of Cas A at 400 Mc/s is assumed to be $S = 56 \times 10^{-24}$ watt/m^2. sterad (c/s) on the basis of the provisional determination reported separately[4]). It is recorded as 514 units (corrected for alinearity and extinction) so that 1 unit equals a flux density of 0.109×10^{-24}.

Further conversion factors depend on the antenna characteristics, which have not yet been measured for the present mirror and feed. Tentatively, we assume the values given in Table 1, where the notations are those of the appendix. The assumed values seem plausible on the basis of the geometry of the antenna and of the values quoted in two recent papers[5]), which are given for comparison.

It now follows (A 26) that 1 unit corresponds to a brightness temperature in the full beam of $0.109 \times 10^{-24}/S_u = 1.57°$K. As noted in the appendix, this conversion factor depends only on h', not on β, which is more uncertain. With the assumed value of β the net antenna temperature corresponding to 1 unit is 1.26°K.

TABLE 1

Assumed antenna characteristics

	H	PT	present paper	units
frequency	3200	600	400	Mc/s
λ	0.094	0.50	0.75	m
$2a$	15.2	11.0	25.0	m
s	0.42	3.3	2.06	degree
f	1.20	1.27	1.20	
c	0.97	1.00	1.09	
h'	0.91	0.79	0.81	
Ω'	0.175	10.9	4.62	sq. degr.
D'	238000	3800	8880	
$10^{24} S_u$	0.17	0.36	0.069	$\frac{\text{watt}}{\text{m}^2\ \text{sterad (c/s)}}$
β	0.28	0.35	0.20	
$h'(1-\beta)$	0.65	0.51	0.65	
D	170000	2500	7100	
$10^{24} S_u/(1-\beta)$	0.23	0.55	0.087	$\frac{\text{watt}}{\text{m}^2\ \text{sterad (c/s)}}$

Stray radiation. The stray radiation received from odd directions, i.e., mainly from the ground, is numerically expressed by the last term of (A 24). Estimating $T_d = 200°$ (about 2/3 ground, 1/3 sky) under average observing conditions and $\beta = 0.20$, it gives a contribution of 40° to the net antenna temperature. This is more than any but the four brightest point sources give (Table 4) and far more than the air radiation in the beam. The stray radiation will vary in an unpredictable manner with the altitude at which the telescope is directed. This makes it essential to make accurate comparison measurements at equal altitude. Our measurements indicated that any systematic changes in the sum of air radiation and stray radiation (last two terms of A 24) were below 8 units (10°K) between $h = 15°$ and $55°$, where most of our observations were made.

[1]) *M.I.T. Rad. Lab. Series* No. 13 (edited by D. E. KERR), Chapter 8, 1951.
[2]) References (A 1) etc. refer to equations in the appendix.
[3]) G. WESTERHOUT, *Radio Astronomy Symposium* 1955, *I.A.U. Symp.* No. 4, Ch. 4, Cambridge Univ. Press, 1957.
[4]) Ch. SEEGER, *B.A.N.* **13**, 100, (No 472), 1956.

[5]) H = F. T. HADDOCK, *Radio Astronomy Symposium* 1955, *I.A.U. Symp.* No. 4, Ch. 33, Cambridge Univ. Press, 1957.
PT = J. H. PIDDINGTON and G. H. TRENT, *Austr. J. Phys.* **9**, 74, 1956.

TABLE 2

Data on isophote maps

		average h of observation	probable NP level in map units	estimated true brightness temperature of o-isophote outside atmosphere
Fig. 1	Cyg-region	34°	0	51°
Fig. 2	Sgr-region	2°.5	—	—
Fig. 3	Tau-region	38°	+ 5	45°
Fig. 4	Ori-region	18°	0	50°

3. *Isophote maps of selected regions*

Four regions have been selected for a reconnaissance by means of systematic azimuth sweeps spaced by about 1°. The results have been worked out in the form of very provisional isophote maps. The co-ordinates are on the equinox of 1956. The intensity in each map is expressed in the units defined in sec. 1. Corrections for alinearity and for extinction have been omitted, except for the Sagittarius map, where an extinction correction of 1.08 was applied to bring the intensities up to the $h = 40°$ level.

The data relating to these maps are given in Table 2. The levels of the isophotes relative to the North pole level have been determined from our own observations and should be correct within about 3 units. They have been corrected for air radiation and converted to brightness temperature (last column) by means of the formula derived in sec. 5.

FIGURE 1

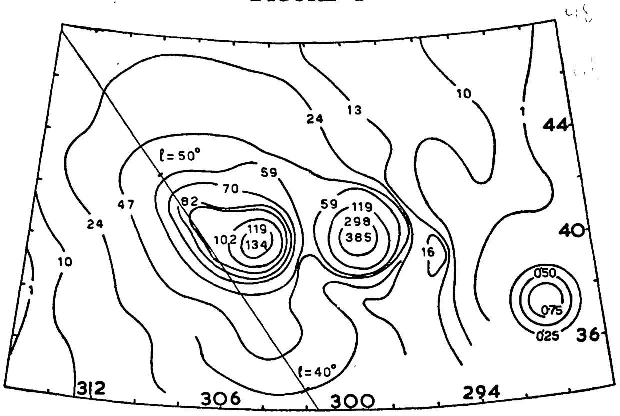

Provisional map of Cygnus region; antenna pattern in lower right corner.

The following comments may be made:
Cygnus region (Figure 1). The map clearly shows the distinction between the two sources that were first separated by REBER and later by PIDDINGTON and MINNETT, whose designations, Cyg A and Cyg X, are commonly used. No other sources are seen with certainty on this map, except for a faint top at $\alpha = 295\frac{1}{2}°$, $\delta = 40°$, which is definitely not a side lobe. The overall distribution shows a ridge along the Milky Way (thin line). The map supports the conclusion drawn by HADDOCK[1]) from observations at 3200 Mc, that Cyg X is not a single source. In our records it seems to consist of a point source at $\alpha = 304°.5$, $\delta = 40°.4$, superposed on one side of an extended source. The point source falls 0°.5 Northwest of the star γ Cyg ($\alpha = 305°.1$, $\delta = 40°.1$). The extended source falls on top of the Milky Way ridge, or is identical with the highest part of this ridge; it is somewhat arbitrary which description we choose. The two positions agree closely to the positions of the two maxima noted by HADDOCK.

A possible separation of the flux densities of the two sources in Cyg X is as follows. The point source rises 68 units above the slanting side of the extended source, giving $S = 7.4 \times 10^{-24}$. The extended source then has a maximum near $\alpha = 307°$, $\delta = 41\frac{1}{2}°$ with a brightness of 87 units above the North pole level. When measured from the 47-unit level, the source has a dimension of $4° \times 3°$ (half-power contour) or $8° \times 6°$ (outer contour), which gives it an apparent solid angle 3 times the antenna pattern, so by (A 28) $g = 3$, giving $S = 13 \times 10^{-24}$. However, it is possible to draw the background under this source at a higher or lower level, as indicated in Table 5. This illustrates the arbitrariness involved in assigning a flux density to such an extended source. A characterization of the spectrum can be given only by comparing isophote maps obtained at various frequencies with not too widely different beam widths. R. D. DAVIES (priv. comm.) finds from such a comparison that the spectrum of Cyg X (total) is essentially flat with $S = 35 \times 10^{-24}$.

Sagittarius region (Figure 2). The discrete source in the direction of the galactic centre at $\alpha = 265°.4$, $\delta = -28°.8$ ($l = 327°.6$, $b = -1°.2$) stands out clearly on top of the galactic ridge, which is at mean galactic latitude $-1°.3$. The isophotes from 160 units down, which are not affected by the source, are remarkably straight. It seems that in the observed region not

[1]) F. T. HADDOCK, *Radio Astronomy Symposium* 1955, *I.A.U. Symp.* No. 4, Ch. 33, Cambridge Univ. Press, 1957.

FIGURE 2

Provisional map of region of galactic centre

FIGURE 3

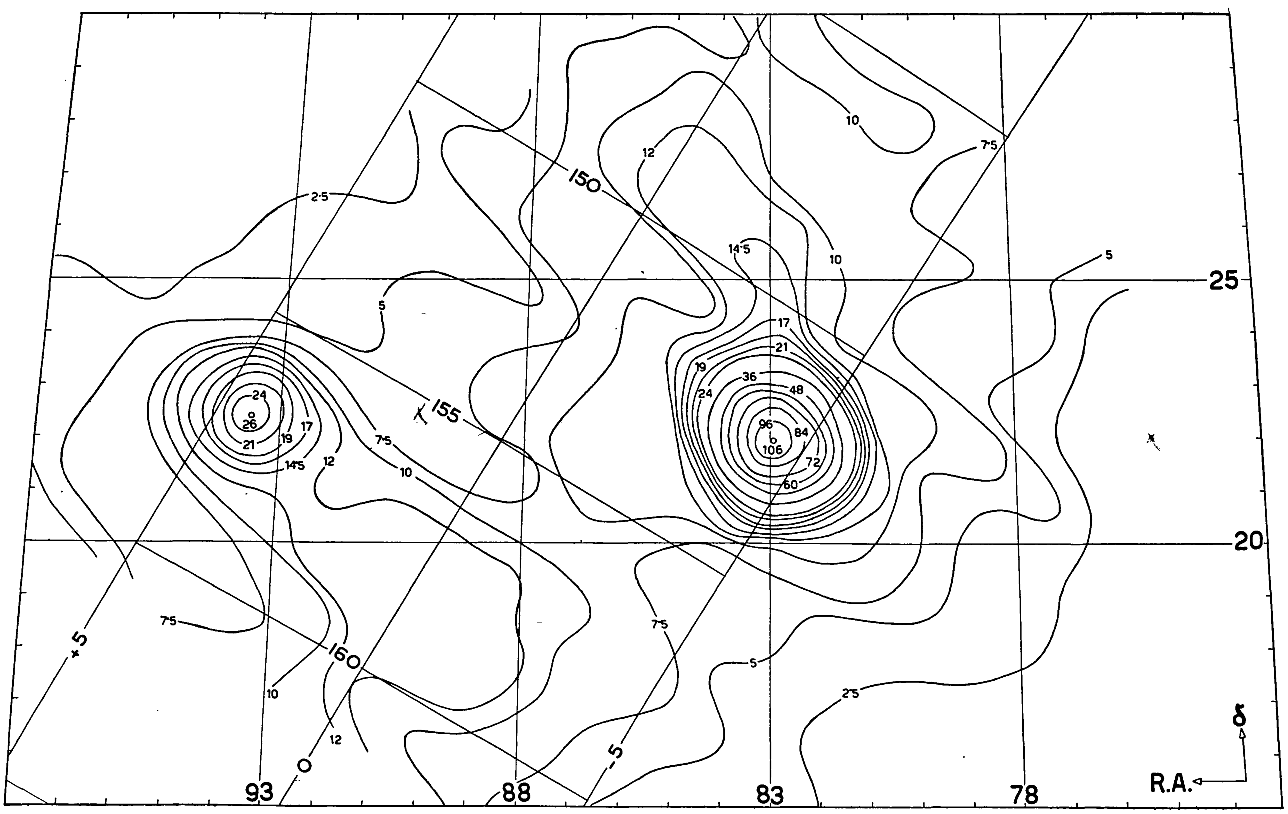

Provisional map of region including the Crab nebula and IC 443 many nearby sources of large size are present. On the assumption that the top of the ridge remains constant at 255 units, the source is found to have a gaussian shape with apparent diameters between half-intensity points of 2°.5 along the galactic plane and 2°.2 at right angles. This corresponds to a true size of about 200 × 100 pc at the distance of the centre. The apparent solid angle is 1.3 times the antenna pattern and the top intensity is 245 units, giving an integrated flux density $S = 35 \times 10^{-24}$.

The comparison with the results of other authors [1]) at the same frequency and with results at 21 cm is made in a separate paper [2]). It is found that the spectrum resembles that of an HII region.

Taurus region (Figure 3). The sweeps through the Crab nebula were combined with sweeps through the source in Gemini associated with the filamentary nebula IC 443. Both sources are at the known positions; the recorded profile of IC 443 is somewhat wider than the beam width. The flux densities are given in Table 4, in which it has been assumed that IC 443 has a true diameter of 1°. The map shows no further sources with certainty. Besides the sources there is again a ridge along the Milky Way with a top of 5 to 7 units above North pole level.

Orion region (Figure 4). Several of the sweeps in the Orion region were continued into the Milky Way.

FIGURE 4

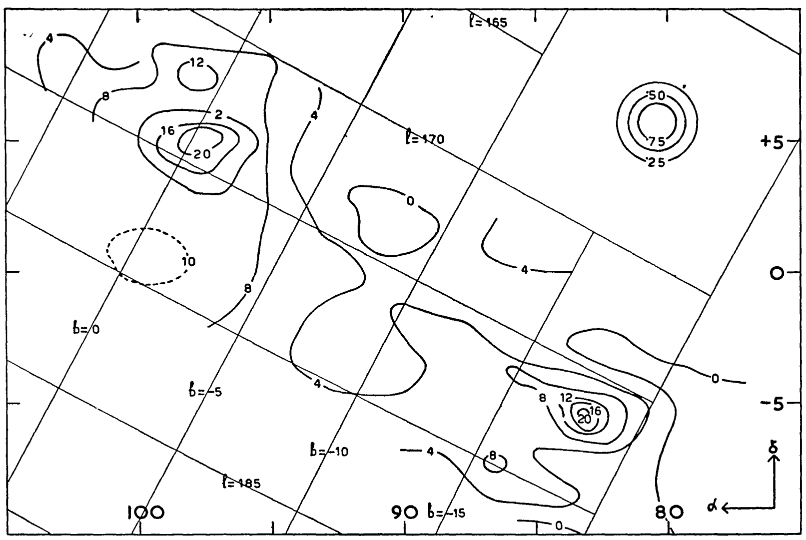

Provisional map of Orion region; antenna pattern in upper right corner.

They covered the Orion nebula ($\alpha = 83°.2$, $\delta = -5°.4$, $b = -18°$) and the Rosette nebula ($\alpha = 97°.5$, $\delta = 4°.9$, $b = 0°$), which has recently been recognized as a radio source [3]). Both nebulae are clearly seen on the map. The Milky Way section near the Rosette nebula was insufficiently covered but suggests again a narrow ridge, possibly with weak sources in it. The intensity between the Orion nebula and the Milky Way is much enhanced over its normal values at $b = -6°$ to $-12°$. Such additional radiation was expected, as this area is covered with faint HII emission. No detailed correspondence with BARNARD's great loop, nor with the intense nebulosity near σ Ori is seen, however.

Andromeda nebula. The Andromeda nebula was just detectable, rising about 4 units above the background.

A rough contour map constructed from the sweeps showed the nebula as a roundish object with an apparent diameter of 2°.8 between half-power points. The resulting flux density, corrected for size, is $S = 0.75 \times 10^{-24}$.

4. *Flux densities of discrete sources*

In addition to the sweeps, a number of observations were made by pointing the antenna at a source and keeping it there for several minutes. This method seemed useful for a rapid intercomparison of the four stronger sources.

Eight intercomparisons of the Cas and Cyg sources were made by alternate settings on these sources with intervals of the order of 5 minutes and with enough North pole readings between them to check on zero drifts. No altitude dependence was detected in the ranges $h = 23°$ to $60°$ for Cas, $h = 10°$ to $49°$ for Cyg, but one Cygnus point at $h = 4°.5$ seemed low by 7 per cent when averaged over the scintillation fluctuations.

[1]) R. X. McGee, O. B. Slee, and G. J. Stanley, *Austr. J. Phys.* **8**, 347, 1955.
[2]) G. Westerhout, *B.A.N.* **13**, 105 (No. 472), 1956.
[3]) H. C. Ko and J. D. Kraus, *Nature* **176**, 221, 1955.

Discarding the latter point we obtained the average uncorrected readings Cas A (at $h = 36°$) = 512 units, Cyg A (at $h = 19°$) = 390 units. Individual readings on either source spread by 10 — 12 units = 2 — 3 per cent. The ratio has a mean error of 1 per cent.

Two further sources, Tau A and Vir A, were measured with similar care. Each of them was compared both to Cas A and to Cyg A in a set of alternate measurements with North pole readings as reference points. The comparison of any two sources was made near a time of equal altitude to avoid differences in extinction or ground radiation. No direct comparison of Tau A and Vir A was possible in the available time. In reducing these data, the interpolated North pole readings were subtracted, the Cas A or Cyg A readings reduced to the standard values 512 and 390, respectively, and proportional correction factors applied to the Tau A or Vir A readings. The final result is shown in Table 3. The agreement between the independent determinations of Tau A and Vir A is quite satisfactory.

TABLE 3
Readings above North pole

	Cas A	Cyg A	Tau A	Vir A
comparison 1	512			29
comparison 2		390	99	
comparison 3		390		31
comparison 4	512		103	

These data require corrections for alinearity of the detector, extinction, and galactic background plus stray radiation, before they can be interpreted in terms of the true ratios of the flux densities from these four sources. Table 4 summarizes this reduction. The initial value of Cyg A (line 3) was averaged between that from the sweeps and that from the comparison measures, which differed by 1.5 per cent. The mean error in line 10 includes the estimated error in the ratio determinations and in the choice of the average background from the isophote maps or sweeps.

TABLE 4
Reduction of point-source data

	Cas A	Cyg A	Tau A	Vir A	
1 source	Cas A	Cyg A	Tau A	Vir A	
2 average h at which observed	36°	19°	45°	36°	
3 reading above NP reference level	512	387	101	30	units
4 alinearity correction factor p	1.048	1.037	1.010	1.003	
5 power above NP level (3×4)	536	401	102	30	units
6 background above NP level from isophote map	26	20	5	−12	units
7 intensity of source seen through air (5 − 6)	510	381	97	42	units
8 extinction ε	0.8	1.4	0.6	0.8	per cent
9 intensity of source outside atmosphere	514	386	98	42	units
10 estimated mean error	±8	±8	±2	±2	units
11 flux density S (mult. 9 by 0.109)	56	42	10.7	4.6	$10^{-24} \frac{\text{watt}}{\text{m}^2\text{c/s}}$
12 net antenna temp. due to source, T_s (mult. 9 by 1.26)	647	486	123	53	°K

Table 5 gives a compilation of the results for all sources observed. M is the maximum reading above the interpolated background in the units used before and reduced to observation outside the atmosphere. The correction factor for size, g, was computed by direct integration of the contours (A 28) for the extended sources Cyg X and the Andromeda nebula. For the smaller sources it was computed from the formula $g = 1 + 0.5\,(2a/s)^2$, which is a compromise between the relation $g = t/(1 - e^{-t}) \approx 1 + \frac{1}{2}t$, with $t = (2a/1.2s)^2$, which holds if the source is a homogeneous disk with diameter $2a$, and $g = 1 + (2a/s)^2$, which holds if the source has a gaussian distribution with diameter $2a$ between half power points. In either formula s is the diameter of the (gaussian) beam between halfpower points. Finally, the flux density was computed from $S = gM \times 0.109 \times 10^{-24}$ watt/m^2.(c/s).

A comparison of these results with those of other authors can best be made by means of a graph of the spectra of these sources. The 400 Mc/s data are in fair agreement with those obtained by the nearest neighbours in frequency, KRAUS and KO[1]) at 250 Mc/s, PIDDINGTON and TRENT[2]) at 600 Mc/s, and DENISSE[3]) at 900 Mc/s. Detailed comments would be premature. The less steep part in the spectra of most sources in the range from 300 to 1000 Mc/s is still

[1]) *Priv. comm.*
[2]) *Austr. J. Phys.* **9**, 74, 1956.
[3]) *Priv. comm.*

TABLE 5

Flux densities of discrete sources at 400 Mc/s

Source	M	g	gM	10^{24} S	
Cas A	514±8	1	514	56.0	
Cyg A	386±8	1	386	42.1	
Tau A	98±2	1	98	10.7	
Vir A	42±2	1	42	4.6	
near-centre source	245±20	1.3	320	35	(narrow source only)
Cyg X1	68	1	68	7.4	(point source)
Cyg X2 (choice)	28	1.4	42	4.6	(extended source)
	40	3	120	13	
	51	5	255	28	
IC 443	19	1.2	23	2.5	
Orion nebula	21	1	21	2.3	
Rosette nebula	12	1.1	13	1.4	
Andromeda nebula	4	1.7	7	0.75	
Moon	3±2	1	3	0.3	

present. The intensity ratios between different sources may vary appreciably in frequency intervals of the order of 50 Mc/s.

The moon was near the limit of detection. The value given in Table 5 corresponds to a brightness temperature of about 90° above the local background, which may have had $T_b = 70°$ (Table 6).

5. *Brightness temperatures of background*

The conversion factor, 1 unit = 1.57°K, found in sec. 2 is subject to (a) the uncertainty in the determination of the flux density of Cas A, on which all absolute values in this paper are based, and (b) the uncertainty in h' (see A 27), which may be about five per cent.

A weakness in the measurements is that no systematic comparisons at equal altitude were made, so that any differences in the stray radiation from one observation to the other have remained uncorrected.

The zero point of the T_b scale can be fixed if we know the brightness temperature of the coldest region in the sky. From sample sweeps at high galactic latitudes we estimated the lowest observed point at − 22 units referred to the NP level; outside the atmosphere this becomes − 24 units. Its true brightness may be estimated in two ways.

(a) MCGEE, STANLEY and SLEE [1]) have tried to determine this temperature (also at 400 Mc/s) by replacing the antenna (including the feed cable) by cold loads. Subtracting the contributions of ground radiation and thermal noise in the feeder and correcting for feeder losses, they arrive at $T_b = 10° \pm 5°$ (p.e.). However, if the uncertainty in the loss factor L mentioned in their paper is also incorporated, the result is $T_b = 10° \pm 21°$. This is the main-beam contribution to the antenna temperature obtained when the antenna is directed at the coldest

[1]) *Austr. J. Phys.* **8**, 347, 1955.

TABLE 6

Brightness temperatures of some regions in the sky

Region	Galactic co-ordinates l	b	r outside atm. (units above NP)	T (°K)
celestial North pole	90°	27°.7	− 1 [1])	52
estimated coldest point	—	~ 90	− 24	16
background Vir A	257.1	74.5	− 14	31
background Orion nebula	176.5	− 18.0	− 3	49
background Tau A	152.3	− 4.3	3	58
background of Moon scans	142.1	18.25	8	66
top of galactic ridge				
near centre	335	− 1.5	—	—
in Cygnus	48	+ 1	30	100
in Monoceros	174	0	10	69
in Taurus	155	0	4	60

[1]) The reference level 0 is the North pole as seen through the atmosphere.

region of the sky. It has to be divided by $1 - \beta$ in order to convert it into the brightness temperature of this region; the value of β is not given.

(b) Extrapolating from the values observed at 100 Mc/s and lower frequencies we might expect that at 400 Mc/s the brightness temperature near the galactic poles might be anywhere from 10° to 25°. The upper limit is supported by DENISSE's determination, $T_b \leq 4°$, made at 900 Mc/s (private communication). The value $T_b = 4°$ at 600 Mc/s assumed by PIDDINGTON and TRENT lies near the lower end of the range of possibilities.
We shall assume that $T_b = 16°$ at 400 Mc/s in the coldest point of the sky. The full relation between r (reading above North pole level in provisional units) and T_b (brightness temperature in °K) then is

$$T_b = 1.57\,(r + 34).$$

The brightness temperatures of other regions, given in Table 6, simply follow from this relation.

6. *Scintillation*

The small time covered by the observations reported here was sufficient to show that scintillation is not restricted to metre wavelengths. Six per cent peak-to-peak fluctuations were recorded on one occasion when observing Cyg A at an altitude of 35°. Below 10°, some scintillation was always present on both Cyg A and Tau A. Figure 5 shows two examples of severe twinkling recorded while observing sources at an altitude of about 4°. Curve (a) shows the fluctuations in the Tau A signal on the afternoon of 2 November. Conditions during the lunar occultation of this source on November 3 were similar. Curve (b) shows the strong and unusually rapid variations in the signal from Cyg A early in the morning of November 4. Twenty-four hours earlier Cygnus A was comparatively steady. At the time of both these observations, Cyg A was close to lower culmination and the radiation passed through the ionosphere in the auroral zone. The Witteveen three-hour K-figures corresponding to these two Cyg A records are 2 and 5 for November 3 and 4, respectively. The high, 12 to 15 "cycle" per minute, fluctuation rate on the later date is in good agreement with the data reported by LITTLE and MAXWELL [1]), who found that the scintillation rate (at longer wavelengths) rises with increasing geomagnetic K-index.

Generally, scintillation on 400 Mc/s appears to be similar in magnitude and form to that found on 200 Mc/s [2]). Furthermore, its magnitude is such that it cannot be ignored in precision observing programs, at least for observatories at the geomagnetic latitudes of Northern Europe and the northern part of the United States.

The observations reported in this paper were made possible by the support of the Netherlands Organisation for Pure Research (Z.W.O.).

FIGURE 5

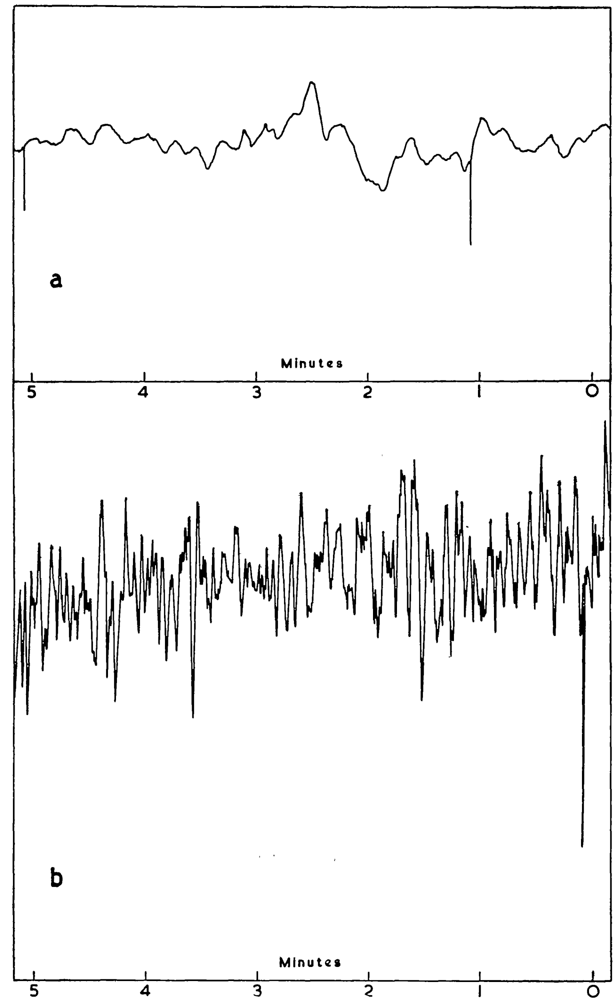

Examples of severe scintillation on 400 Mc/s.

Curve (a) — 2 Nov, 1955, Tau A at 4° altitude in the north-west, recording time constant 1^s.

Curve (b) — 4 Nov. 1955, Cyg A at 4° altitude near lower culmination. The electrical time constant was $0^s.1$, but the fluctuations may have been somewhat smoothed by the response of the recording potentiometer, whose pen required about one second for full-scale deflection.

The receiver was adjusted to different sensitivities for these two observations. The time axis corresponds to zero intensity.

1) C. G. LITTLE and A. MAXWELL, *Atm. Terr. Physics* **2**, 356, 1952.

2) C. L. SEEGER, *J. Geoph. Res.* **56**, 239, 1951.

APPENDIX

TERMS AND FORMULAE FOR PENCILBEAM ANTENNAS

The concepts and formulae needed in the reduction of observations made with very narrow beams are scattered in the literature and are sometimes used inconsistently. For this reason a new summary of the principal terms and relations seemed desirable.

1. *Antenna specifications*

1. In a transmitting antenna, the power transmitted in the direction (θ, φ) in both polarizations together is proportional to $f(\theta, \varphi)$. When the same antenna is used as a receiving antenna, the power received from a distant unpolarized source in the direction (θ, φ) is proportional to the same $f(\theta, \varphi)$. The function $f(\theta, \varphi)$ will be normalized by putting $f = 1$ at the centre of the beam $(\theta = 0)$.

2. Let the term *full beam* mean the main beam and its adjoining side lobes, or, if there are no minima in the pattern, its wings. As a precise definition we propose that the full beam should be enclosed by the circle with diameter 5 times the halfpower diameter (or beam width). In a theoretical pattern "full beam" may be interpreted to mean the full diffraction pattern, with an error not exceeding a few per cent.

3. We define the ratio

$$\beta = \int_{\substack{\text{sphere}\\ \text{minus}\\ \text{full beam}}} f(\theta, \varphi)\, d\Omega \Big/ \int_{\text{sphere}} f(\theta, \varphi)\, d\Omega, \qquad \text{(A 1)}$$

and call β *stray factor*, or the *wide-angle fraction*. The radiation (received or transmitted) in directions not in the full beam may be called *stray radiation* by a term borrowed from optical astronomy; it simply means any unwanted radiation in odd directions. In a common radiotelescope the non-zero value of β is due to spill-over, scattering against feed and feed supports, and radiation through the reflecting screen.

Note: The need for introducing this parameter has arisen by the use of antennas with narrow beams, where the integral over the wide-angle lobes may be appreciable in spite of the fact that the sensitivity is very much smaller there than in the main beam.

4. Two closely related quantities are defined by

$$D' = \frac{4\pi}{\int_{\text{full beam}} f(\theta, \varphi)\, d\Omega}, \qquad \text{(A 2)}$$

$$D = \frac{4\pi}{\int_{\text{sphere}} f(\theta, \varphi)\, d\Omega}. \qquad \text{(A 3)}$$

They are related by

$$D = (1 - \beta) D'. \qquad \text{(A 4)}$$

We shall call D the *directivity* (standard term) and D' *beam directivity* [1]). Neither quantity can be readily dispensed with. The quantity D' is more easily measurable or calculable and plays the prominent role in comparing observations of point sources and of extended regions (see A 26). The quantity D is more fundamental and more directly related to the gain and effective area (see A 6).

The integral in the denominator of (A 2) will be called the *effective solid angle* of the beam and will be denoted by Ω'. Thus

$$\Omega' = 4\pi/D' \text{ steradians} = 41253/D' \text{ sq. degrees.} \qquad \text{(A 5)}$$

5. The *gain G* with respect to an isotropic radiator is most easily defined in terms of a transmitting antenna by the usual definition:

$$G = \frac{\text{radiation intensity from antenna in direction of maximum}}{\text{radiation intensity from lossless isotropic radiator with same power input}}.$$

The gain thus defined includes the loss factor L in dielectrics and conductors of the transmission lines. It is related to directivity by

$$G = LD = L(1 - \beta) D'. \qquad \text{(A 6)}$$

Compared with the directivity, it contains only the cable loss; compared with the beam directivity it contains both the cable loss and the loss due to stray radiation.

6. The *effective area A* of the antenna is defined as the available power at the receiver input terminals when the antenna is exposed to a plane wave of unpolarized radiation in the main direction divided by half the power per unit area carried by this wave. It is universally related to the gain by

$$A = \frac{\lambda^2}{4\pi} \cdot G. \qquad \text{(A 7)}$$

7. A mirror with diameter $2a$ has the *geometrical area*

$$A_g = \pi a^2. \qquad \text{(A 8)}$$

Whenever a well defined geometrical area exists the *antenna efficiency h* is defined by

$$h = A/A_g = \frac{\lambda^2}{4\pi A_g} \cdot G. \qquad \text{(A 9)}$$

If we define the *diffractive efficiency* of the antenna in an analogous manner by

$$h' = \frac{\lambda^2}{4\pi A_g} \cdot D', \qquad \text{(A 10)}$$

then

$$h = L \cdot (1 - \beta) \cdot h'. \qquad \text{(A 11)}$$

[1]) Called "nominal gain" by PIDDINGTON and TRENT (*Austr. J. Phys.* **9**, 74, 1956) and "diffractive gain" by HADDOCK (in correspondence).

The antenna efficiency is thus made up of three factors, each < 1.

8. The diffractive efficiency just defined may be simply calculated for a uniphase circular current sheet in which the field is tapered as $g(\rho)$, the power as $g^2(\rho)$, $0 < \rho < a$, $g(0) = 1$. The result is

$$h' = I_1^2/I_2\,, \qquad \text{(A 12)}$$

$$\text{with } I_1 = \frac{1}{a^2}\int_0^a g(\rho)\,2\rho\,d\rho\,,\quad I_2 = \frac{1}{a^2}\int_0^a g^2(\rho)\,2\rho\,d\rho.$$

A fairly flexible assumption is $g = 1 - q(\rho/a)^n$, which gives

$$I_1 = 1 - \frac{2q}{n+2},\qquad I_2 = 1 - \frac{4q}{n+2} + \frac{q^2}{n+1}. \qquad \text{(A 13)}$$

The parameters $n = 2$, $q = 2/3$ give an illumination closely resembling a cosine-tapered illumination down 10 db at the edge. The resulting values are $I_1 = 2/3$, $I_2 = 13/27$, $h' = 0.92$.

9. The *beam widths*, s_a and s_b, are the angles in degrees in the two main planes between half-power points. They are inconvenient in theory but convenient in measurement. Let us write $s^2 = s_a s_b$ and define the factor c by

$$\Omega'\,(\text{square degrees}) = c\,s^2. \qquad \text{(A 14)}$$

It then follows that

$$D' = \frac{41253}{c\,s^2}\,,\quad D = (1-\beta)\,\frac{41253}{c\,s^2}\,,\quad G = L(1-\beta)\,\frac{41253}{c\,s^2}. \qquad \text{(A 15)}$$

The factor f may be defined by

$$s = \sqrt{s_a s_b} = 57^\circ.3\,\frac{\lambda}{2a}\cdot f. \qquad \text{(A 16)}$$

It then follows from (A 5, A 8, A 10, A 14, A 16) that

$$h'\,.\,c\,.\,f^2 = 4/\pi. \qquad \text{(A 17)}$$

All factors in (A 17) depend on the shape of the beam only and are unaffected by stray radiation.

10. *Suggested measurements.*

A consistent reduction of the data obtained with a particular instrument requires a set of measurements as follows.

Antenna pattern of the main lobe and the adjoining side lobes; to be measured by scanning the sun, a strong point source, or an artificial point source. From it we find Ω', D' (A 5 and A 2), s_a, s_b, s, h', c, f (A 10, A 14, A 16), check (A 17).

Loss in cable, by standard method, gives L.

The remaining data may be found in either [1]) of two ways:

(a) Measure antenna pattern over entire sphere (quite difficult). Find β and D (A 1, A 3), G, A, and h (A 6, A 7, A 9), check (A 11).

(b) Measure G by comparing the antenna with an antenna (horn) of calculable gain. Then again D, A, h, β (A 4, A 6, A 7, A 9) and cross checks.

2. *Observation of sources*

1. The *brightness B and brightness temperature* T_b at any frequency and at any point of the sky (emitting unpolarized radiation) are related by

$$B = 2k\,T_b/\lambda^2, \qquad \text{(A 18)}$$

where k is the Boltzmann factor.

A discrete source is characterized by B or T_b as a function of the celestial co-ordinates. The integral

$$S = \int_{\text{source}} B\,d\Omega \qquad \text{(A 19)}$$

is the *flux density*.

A *point source* occupies such a small solid angle that the antenna sensitivity does not vary over the entire source, when the source is centered on the beam. An *extended source* is any source that is not a point source.

2. By *net antenna temperature* T_a we shall understand the antenna temperature measured at the feed, i.e. avoiding cable losses. By *gross antenna temperature* T_a^* we shall understand the antenna temperature measured at the receiver input terminals. The relation is

$$T_a^* = L\,T_a + (1-L)\,T_c\,, \qquad \text{(A 20)}$$

where L is the loss factor defined before and T_c is the temperature of the cable ($\approx$ ambient temperature).

3. Let in any direction above the horizon, ε be the power fraction lost by extinction in the air. The observed brightness in that direction is then described by the temperature

$$T'_b = T_b - \varepsilon\,T_b + \varepsilon\,T_0\,, \qquad \text{(A 21)}$$

where T_0 = average air temperature along the path. To a good approximation $\varepsilon = 1 - p^{\operatorname{cosec} h}$, where p is power transmission factor for a source at the zenith and h = altitude. Near the horizon ($h < 10^\circ$) a more precise formula is needed. We shall call T'_b the *apparent brightness temperature* and T_b *the true brightness temperature*. The positive correction term in (A 21) describes the *air radiation*, the negative term the *extinction*.

4. It follows from the preceding definitions that with an arbitrary distribution of sources for the an-

[1]) If L is made up of losses in many components and cannot readily be measured, both methods may be used to find D and G. Then L is defined by (A 6).

tenna pointing in an arbitrary direction the net antenna temperature is given by

$$T_a = \frac{D}{4\pi} \int_{\text{sphere}} f(\theta, \varphi)\, T'_b\, d\Omega. \qquad \text{(A 22)}$$

Suppose that an observation could be made with no air and only one point source of flux density S observed at the centre of the beam; T_a then would by (A 18, A 19, A 21, A 22), with $\varepsilon = 0$ and $f(\theta, \varphi) = 1$, assume the value

$$T_a = T_s = \frac{\lambda^2}{8\pi k} D\, S. \qquad \text{(A 23)}$$

Now, suppose that an observation is made while (a) the same point source is at the centre of the beam shining through the air, (b) an even background of true brightness temperature T_b is present in the "full beam", effectively shining through the same amount of air, (c) an average apparent brightness temperature T_d is seen in all further directions of the sphere. The net antenna temperature then is

$$T_a = (1 - \varepsilon)\, T_s + (1 - \varepsilon)(1 - \beta)\, T_b + \varepsilon(1 - \beta)\, T_0 + \beta\, T_d. \qquad \text{(A 24)}$$

If $T_s = 0$ and $T_b = T_d = T_0$, then also $T_a = T_0$, as it should be on thermodynamic grounds.

5. An increase of 1° in T_a may (by A 22—24) be brought about by an increase of

$$\left.\begin{array}{l} 1^\circ \text{ in } T'_b \text{ over entire sphere} \\ \dfrac{1^\circ}{(1-\varepsilon)(1-\beta)} \text{ in } T_b \text{ over full beam} \\ \dfrac{8\pi k}{(1-\varepsilon)\lambda^2 D} \text{ in } S \text{ at centre of beam} \end{array}\right\} \text{equivalent} \qquad \text{(A 25)}$$

With the aid of (A 4) it follows that equal increase in the recorded intensity is given by an increase of

$$\left.\begin{array}{l} 1^\circ \text{ in } T_b \text{ over full beam} \\ \dfrac{8\pi k}{\lambda^2 D'} \text{ in } S \text{ at centre of beam} \end{array}\right\} \text{equivalent} \qquad \text{(A 26)}$$

The expression in (A 26) will be denoted by S_u and may by (A 10) be written in the form

$$S_u = \frac{8\pi k}{\lambda^2 D'} = \frac{2k}{h' A_g},$$

or in mks units

$$10^{24} S_u = \frac{347}{\lambda^2 D'} = \frac{27.6}{h' A_g}. \qquad \text{(A 27)}$$

6. *Suggested reduction methods*

If absorbed powers are recorded on an unknown scale and one point source of known S is available, the S of other point sources is found in proportion, and the T_b of extended regions (i.e. regions in which the brightness changes slowly over the beam width) is found from the rule that 1°K corresponds to the flux density S_u (A 27). Neither T_a nor β enter into the reduction.

If an absolute calibration of the receiver can be made, T_a^* can be determined and from it T_a (A 20). After extinction correction, 1° in T_a corresponds to $1^\circ/(1 - \beta)$ in T_b (A 25). An evaluation of the stray radiation (last term in A 24) is required in order to determine the zero of the T_b-scale. The scale of flux densities follows from that of T_b by (A 27) or from that of T_a by (A 25).

The S of an extended source may be determined from full scans across it in either of two ways: (A) Determine T_b at each point by the previous methods, not minding distortion by the finite beam width, and integrate (A 18, A 19); (B) Determine a value of S' from the maximum reading as if it were a point source and apply a *correction factor for size* equal to

$$g = \frac{\text{apparent solid angle of source}}{\text{effective solid angle of beam } (= \Omega')}, \qquad \text{(A 28)}$$

where the denominator is defined earlier (A 2, A 5) and the numerator is defined as the integral over the source divided by the maximum reading. Both methods should give identical results. If full scans are not available, g may be calculated from an assumed size and brightness distribution of the source.